The Wave Filter Design of UFMC Vehicle Communication System

Tengyue Yu(✉), Jingjing Wang, Jiangang Wen, Feng Li, and Jingyu Hua

School of Information and Electronic Engineering, Zhejiang Gongshang University, Hangzhou 310018, China
19020090017@pop.zjgsu.ecu.cn

Abstract. In recent years, the requirements for low delay and reliability of vehicular communication are becoming more and more strict, while the traditional OFDM (Orthogonal Frequency Division Multiplexing) technology can not meet the above requirements due to high out-of-band leakage and strict synchronization requirements. Therefore, in this paper, the UFMC (Universal filtered multi carrier) system is applied to the Internet of vehicles communication, and the overall performance of the system is improved through the optimization design of the waveform filter. The simulation results show that the FIR (finite impulse response) filter designed in this paper can improve the SER (symbol error rate) performance of UFMC system compared with DC (Dolph Chebyshev) filter.

Keywords: Vehicle communication · UFMC · FIR filter · SER

1 Introduction

With the official commercial use of 5G and the popularization of mobile terminal equipment, people gradually have a deeper understanding of the concept of Internet of things. Three technology scenarios are defined in 5G, which are eMBB (Enhanced Mobile Broadband), uRLLC (Ultra Reliable and Low Latency Communication) and mMTC (Massive Machine Type of Communication). Among them, uRLLC can satisfy millisecond level and end-to-end low delay transmission [1,2], which promotes the development of a large number of delay sensitive mobile applications, such as realtime navigation and autopilot [3,4]. VANET (Vehicular Ad-hoc Networks), referred to as the Internet of vehicles, is one of the important applications of 5G system in high reliability and low delay communication scenarios. The Internet of vehicles uses advanced sensor technology, cloud computing technology, wireless communication technology, etc., which can fully sense the realtime situation of road and traffic, and connect a certain range of vehicles, pedestrians and roads to form a special mobile Ad-hoc network [5]. At present, a large number of 5G base stations are integrated into the Internet

X. Jiang (Ed.): MLICOM 2021, LNICST 438, pp. 67–78, 2022.
https://doi.org/10.1007/978-3-031-04409-0_7

of vehicles, which makes the technology of security authentication, interference management and load balancing have further development. To a certain extent, it greatly alleviates the traffic pressure and improves the travel safety.

In the Internet of Vehicles, V2V (Vehicle to Vehicle) communication, V2P (Vehicle to Pedestrian, Vehicle to Person) and other communication services require faster and more reliable information in the transmission process, which puts forward new requirements for basic waveforms [6,7]. If thousands of connections in the Internet of Vehicles scene use the strictly synchronized OFDM system, a large amount of synchronization signaling will appear in the network, which will cause network congestion [8]. As a new multi carrier technology, UFMC suppresses the out of band leakage by filtering the sub-band, so as to reduce the small frequency offset interference and has low synchronization requirements [9]. UFMC uses shorter filter length, which is more suitable for short burst packet transmission with low power consumption [10], such as cognitive M2M (Machine to Machine) communication [11]. These advantages make UFMC system more suitable for vehicle communication.

The current research on UFMC have been carried out. Paper [12] introduces the system model and system principles of UFMC, and analyzes the channel's influence on UFMC when CFO (carrier frequency offset) exists, and at the same time, the robustness of the system against CFO is improved by optimizing the filter parameters. Paper [13] proposes to use two different optimization criteria to optimize the design of FIR filters. The first is to maximize the ratio of signal to out-of-band leakage, and the second is to maximize the ratio of signal and in-band distortion plus out-of-band leakage. The filter optimized by these two criteria can effectively improve the SIR (Signal to Interference) of the system. Paper [14] considers time and frequency offset on the basis of paper [13]. Compared with the UFMC system using DC filtering, the SIR of the optimized UFMC system is increased by 3.6 dB, compared with the traditional OFDM system, the SIR of the optimized UFMC system is increased by 15.1 dB. Paper [15] uses Chebyshev filter, Hamming filter and Hamming filter to filter the UFMC system. The results show that UFMC system is superior to OFDM signal in side lobe attenuation, bit error rate and error vector amplitude. Paper [16,17] proposed a pilot design method to suppress the interference in the UFMC system and effectively reduce the system's bit error rate. Paper [18] proposed a convex optimization method to optimize the filter, and the optimized filter can suppress out-of-band interference to the maximum extent.

Based on the above analysis, it is found that researchers have made some achievements in the research of UFMC system, but most of the researches are based on suppressing the interference of UFMC system, lack of research on the relationship between filters index and system SER. This paper will conduct in-depth research on this problem. Firstly, according to the basic principle of UFMC system, the signal expression after AWGN (Additive White Gaussian Noise) channel is derived, and the interference situation is analyzed. Then the FIR filter is designed according to the CMM (constrained minimum maximum) criterion, and the SER of UFMC system under each index is obtained by traversing the filters index, and the relationship between the filters index and SER is analyzed. Finally, the results show that the FIR filter designed in this paper can improve the SER performance of UFMC system compared with the UFMC system using DC filter.

2 Signal Model of UFMC System

2.1 Transmitter Model of UFMC System

The system model of UFMC is shown in Fig. 1. The overall bandwidth is divided into B sub-bands, and each sub-band can be allocated N_B sub-carriers. With the N-point IDFT operation, the frequency domain signal X_i after equalization is transformed into time domain x_i. Then this output signal is filtered by a filter f_i with the length of L. That results in a symbol length of $N+L-1$ because of the linear convolution between x_i and f_i.

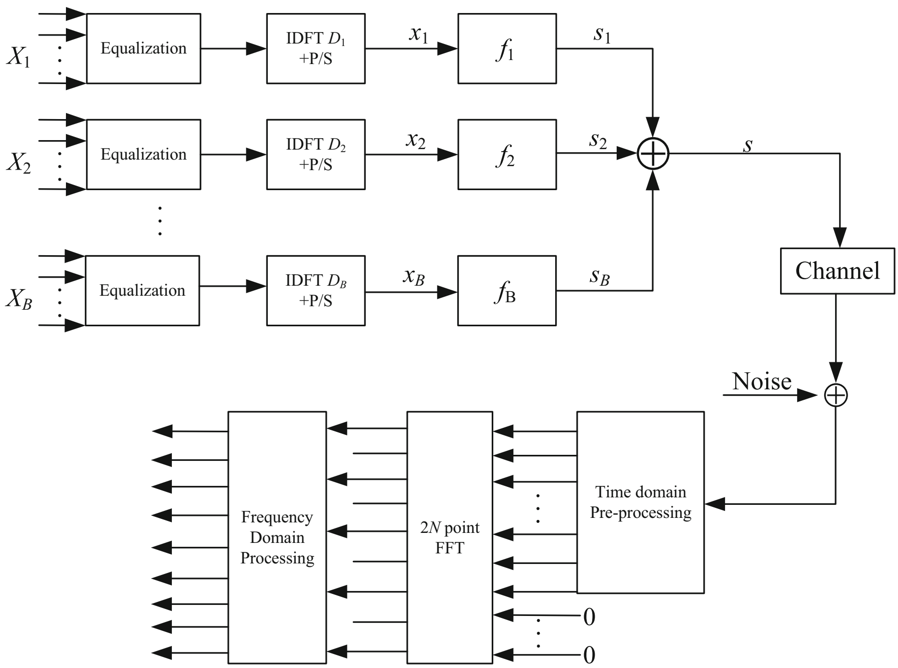

Fig. 1. UFMC system model

Finally, all the filtered sub-band signals $\mathbf{s}_i$ are added together and transmitted. The transmitted signal $\mathbf{s}$ can be expressed as:

$$\mathbf{s} = \sum_{i=0}^{B-1} \mathbf{F}_i \mathbf{V}_i \mathbf{E}_i \mathbf{X}_i \tag{1}$$

where $\mathbf{X}_i$ is a matrix which the element is the signal to be modulated on the i-th sub-band; $\mathbf{E}_i$ is a equalization matrix, where the element is the reciprocal of the amplitude frequency response of the sub-band filter on the current subcarrier; $\mathbf{V}_i$ is the N-point IDFT matrix with the size of $N \times N_B$. The k-th row and n-th column element of $\mathbf{V}_i$ is $\frac{1}{\sqrt{N}} e^{j2\pi \frac{(k-1)[(i-1)\times N_B+n-1]}{N}}$. $\mathbf{F}_i$ is a Toeplitz matrix with its first column being $\left[f_k(0), f_k(1), \ldots, f_k(L-1), 0_{1\times(N-1)}\right]^T$, and first row being $\left[f_k(0), 0_{1\times(L-1)}\right]^T$.

2.2 Derivation of SINR in UFMC System

Considering that the channel is AWGN channel and is affected by CFO, the received time domain signal $\mathbf{r}$ can be expressed as:

$$\mathbf{r} = \mathbf{\Gamma}(\varepsilon)\mathbf{FVEX} + \mathbf{z} \tag{2}$$

where, ε represents the normalized carrier frequency deviation, $\mathbf{z}$ represents the additive white noise in the channel, and the remaining matrices are expressed as follows:

$$\mathbf{X} = \left[\mathbf{X}_1^T, \mathbf{X}_2^T, \ldots, \mathbf{X}_B^T\right]^T \tag{3}$$

$$\mathbf{E} = \mathrm{diag}\left[\mathbf{E}_1, \mathbf{E}_2, \ldots, \mathbf{E}_B\right] \tag{4}$$

$$\mathbf{V} = \mathrm{diag}\left[\mathbf{V}_1, \mathbf{V}_2, \ldots, \mathbf{V}_B\right] \tag{5}$$

$$\mathbf{F} = \left[\mathbf{F}_1, \mathbf{F}_2, \ldots, \mathbf{F}_B\right] \tag{6}$$

$$\mathbf{\Gamma}(\varepsilon) = \mathrm{diag}\left[1, e^{j2\pi\frac{\varepsilon}{N}}, \ldots, e^{j2\pi\frac{\varepsilon(N+L-2)}{N}}\right] \tag{7}$$

At the receiver, FFT-based detection is used to transform the received time domain signal into frequency domain. Since the UFMC symbol has the length $N+L-1$, zeros are padded to perform the 2N-point FFT. Finally, the frequency domain expression of the signal can be expressed as:

$$\mathbf{Y} = \mathbf{D\Gamma}(\varepsilon)\mathbf{FVEX} + \mathbf{Z} \tag{8}$$

where $\mathbf{D}$ is a 2N-point DFT matrix with the size of $N \times N + L - 1$, and the k-th row and n-th column element can be expressed as $\frac{1}{\sqrt{N}} e^{j2\pi\frac{2(k-1)(n-1)}{N}}$.

Let:

$$\mathbf{Q} = \mathbf{D\Gamma}(\varepsilon)\mathbf{FEV} \tag{9}$$

For the k-th subcarrier, the useful signal can be expressed as $Q(k,k)X(k)$, the interference signal can be expressed as $\sum\limits_{m\neq k} Q(k,m)X(m)$, then the SINR expression of the k-th sub-carrier can be written as:

$$\mathrm{SINR}_k = \frac{Q^H(k,k)Q(k,k)}{\sum\limits_{m\neq k} Q^H(k,m)Q(k,m) + Z^H(k)Z(k)} \tag{10}$$

3 Design of Waveform Filter

3.1 Filter Optimization Design Model

It can be seen from formula (11) that in order to reduce the SER of the system, it is necessary to suppress interference signals through filters as much as possible. In the design of linear phase filters, CMM criterion is usually considered. In the CMM criterion, it is planned to consider maximum stop-band attenuation of filter, and constraining the pass-band ripple. The mathematical model can be expressed as:

$$\min_{\mathbf{x}} \mathbf{c}_s^T \mathbf{x}$$
$$\text{s.t.} \begin{cases} 1 - \mathbf{c}(\omega)^T \mathbf{x} \leq \delta_p^l, \omega \in [0, \omega_p] \\ \mathbf{c}(\omega)^T \mathbf{x} - 1 \leq \delta_p^u, \omega \in [0, \omega_p] \end{cases} \tag{11}$$

where $\mathbf{x} = \left[\hat{\mathbf{h}}^T, \delta_s\right]^T$, $\mathbf{c}_s = \begin{bmatrix} \mathbf{0}_{N\times 1} \\ 1 \end{bmatrix}$, $\mathbf{c}(\omega) = \left[2\cos\left(\omega\left(\frac{L-1}{2}\right)\right), \cdots, 2\cos(\omega), 1\right]^T$, $\mathbf{h}$ is the filter coefficient, δ_p^l represents the lower bound of the pass-band ripple, and δ_p^u represents the upper bound of the pass-band ripple.

The filter design model of formula (11) can flexibly adjust the target requirements to meet special requirements. Figure 2 shows an example, Compared with the DC filter, the FIR filter has a smaller attenuation in the pass-band, and the transition-band is longer than DC, which means that the attenuation of the filter designed in this paper is slower than that of the DC filter in the transition-band.

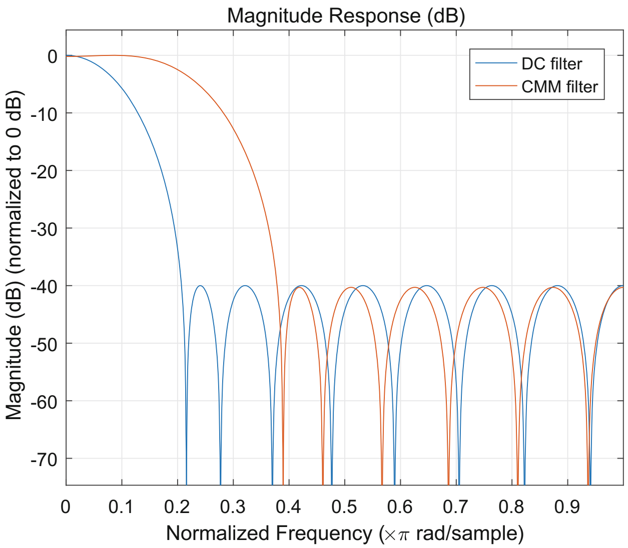

Fig. 2. Magnitude response comparison of DC filter and FIR

3.2 Influence of Filter on Subcarrier Interference of UFMC System

Figure 3 show the comparison of SINR in a sub-band of UFMC system using DC filter and FIR filter of Fig. 2 when CFO = 0 and 0.05. The simulation results show that when CFO = 0, the SINR of each sub-carrier is equal, and the gain of FIR filter is small compared with that of DC filter. When CFO = 0.05, the SINR of the middle sub-bands are lower than that of the edge sub-bands. The SINR of the middle sub-bands of FIR filter is about 1 dB higher than that of the DC filter, but it is lower than that of the edge sub-bands.

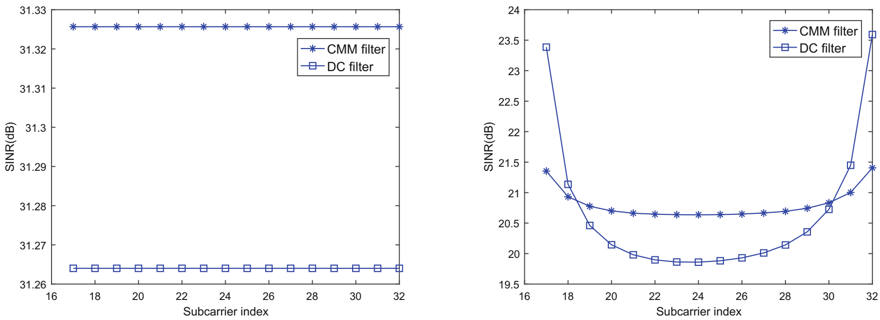

(a) CFO = 0 (b) CFO = 0.05

Fig. 3. Performance comparison of DC filter and FIR filter

Figure 4 show the comparison of SINR in a sub-band of UFMC system when FIR filters with different pass-band ripple are used at CFO = 0 and 0.05. The simulation results show that when CFO = 0, the SINR of each sub-carrier is equal, and the change of pass band fluctuation has little effect on the system gain. When CFO = 0.05, the smaller the pass-band ripple of the filter is, the SINR of the sub-carriers in the middle of the sub-bands can be improved. In addition, the smaller the pass-band ripple of FIR filter is, the smaller the stop-band fluctuation is, the slower the transition-band drops, and the worse the interference suppression to the edge sub-carriers, resulting in the worse SINR of the edge sub-carriers.

From the above analysis, it can be found that the filters index can affect the performance of UFMC system. According to the amplitude response comparison of DC filter and FIR filter, it can be inferred that the smaller the pass-band ripple is, the smaller the interference of the intermediate sub-carriers is; The more slowly the transition-band decays, the more interference the edge sub-carriers suffer. In view of the above ideas, this paper intends to use the method of traversing index to find a more suitable waveform filter for UFMC system through the comparison of SER.

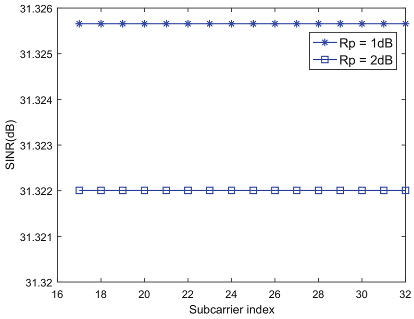

(a) CFO = 0

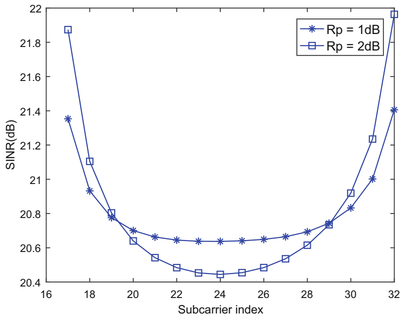

(b) CFO = 0.05

Fig. 4. Performance comparison of FIR filter with different pass-band ripples

4 Simulation Results and Analysis

The relevant simulation parameters used in this paper are shown in Table 1:

Table 1. Simulation parameter

Parameter	Value1	Value2
Number of sub-carriers	96	96
Number of sub-bands	6	6
FFTsize	128	128
Modulation	16QAM	16QAM
SNR	15 dB	30 dB
CFO	0	0.05

4.1 Performance Analysis of Filter Index Under Large Step Size

The traversable table under large step is shown in Table 2:

Table 2. Traversable table under large step size

Filter parameters	Value
The length of filter	25
The pass-band/stop-band cut-off frequency of filter	0.125/0.2
The pass band ripple of filter	[1 dB:1 dB:6 dB]

Figure 5 shows the SER curves of UFMC system by using FIR filters with different pass-band ripples and the SER curves of UFMC system with DC filters.

It can be seen from the figure that when CFO is 0, there is little difference between the performances of different filters. This phenomenon indicates that when CFO = 0, the interference caused by CFO is very small, and no matter what kind of filter is used, there is little difference in SER. When CFO = 0.05, it can be seen from the figure that with the increase of pass-band ripple, the SER performance of the system is on the rise. In addition, the minimum SER of the filter designed in this paper is less than that of the DC filter.

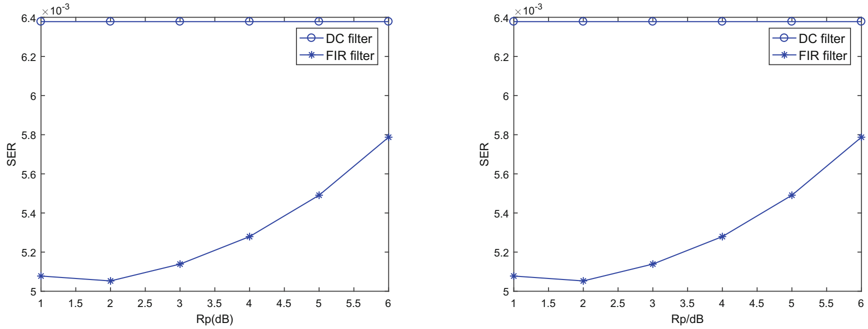

(a) CFO = 0 (b) CFO = 0.05

Fig. 5. SER comparison of UFMC systems with different filters

As can be seen from Fig. 6, with the increase of pass-band ripple, the SER of the intermediate carrier is gradually increasing. As the pass-band ripple increases, the filter stop-band attenuation can be improved. At this time, the filter in the transition-band will attenuate faster, and the interference suppression effect on the edge sub-carriers are better, so the SER on the edge-subcarriers are lower.

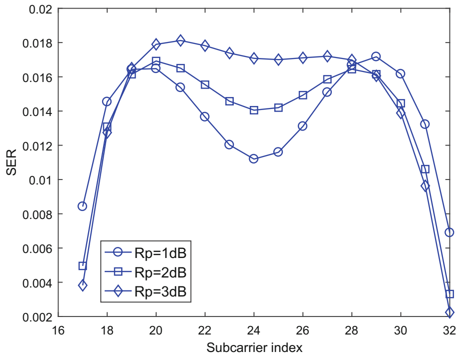

Fig. 6. SER comparison of each subcarrier under different pass-band ripples

4.2 Performance Analysis of Filter Index Under Small Step Size

Section 4.1 analyzes the influence of filter index on SER of UMFC system in large step size. Based on Sect. 4.1, this section narrows the search interval and continues to search for the filter with good performance in small step size. The traversable table is shown in Table 3:

Table 3. Traversable table under small step size

Filter parameters	Value
The length of filter	25
The pass-band/stop-band cut-off frequency of filter	0.125/0.2
The pass band ripple of filter	[0.1 dB:0.1 dB:1 dB]

Figure 7 shows the performance of UFMC system with small step length to traverse the filter pass-band ripple when CFO = 0.05. It can be seen that as the pass-band ripple continues to decrease, the SER is not greatly improved, which indicates that in UFMC system, there is a threshold for the filter pass-band ripple to improve the system performance. Even if the pass-band ripple continues to improve, the performance of UFMC system will not be better, or even worse.

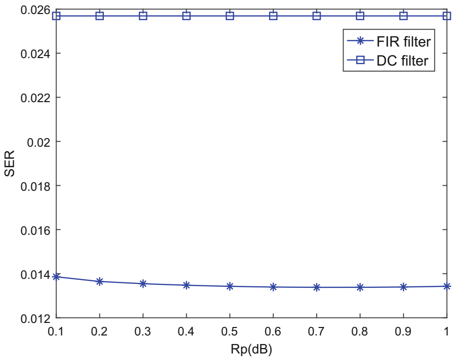

Fig. 7. SER comparison of UFMC systems with different filters

As can be seen from Fig. 8, when the pass-band ripple is 0.1 dB, the SER of the edge subcarrier is the worst, because the pass-band ripple of the filter is the smallest, the stop-band fluctuation of the filter becomes smaller. At this time, the transition-band attenuation is the slowest, so that the interference suppression to the edge sub-carrier is the worst. In addition, the SER of the intermediate-carrier is not improved, which leads to the increase of the overall SER.

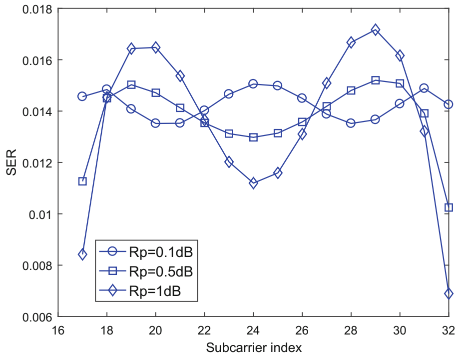

Fig. 8. SER comparison of each subcarrier under different pass-band ripples

4.3 Performance Comparison

It can be seen from Sect. 4.1 and 4.2 that the best filter for UFMC system performance is FIR filter with 1 dB pass band ripple. Figure 9 show that the performance of the FIR filter designed in this paper is better than that of the DC filter in UFMC system regardless of the modulation order with or without CFO.

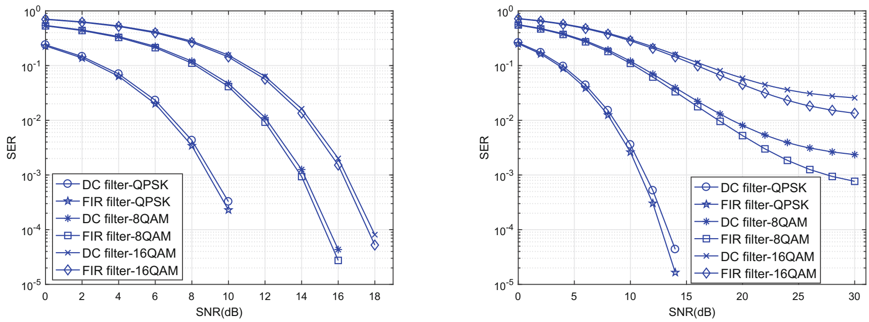

(a) CFO = 0 (b) CFO = 0.05

Fig. 9. SER comparison of FIR filter and DC filter

5 Conclusion

Aiming at the problem that the Internet of vehicles is sensitive to time delay and synchronization, this paper proposes to apply UFMC system to the Internet of vehicles. In order to improve the reliability of UFMC system, this paper analyzes the problem of inter-carrier interference in UFMC system, and gives the detailed derivation process. Then, the interference is suppressed by optimizing the design of waveform filter. The performance of UFMC system using FIR filter and DC filter is compared by MATLAB simulation platform in AWGN channel with or without CFO, The influence of filter index on the performance of UFMC system is analyzed. The results show that the waveform filter designed in this paper is better than the DC filter to a certain extent, and can effectively improve the reliability of the system.

References

1. Li, B., Fei, Z., Zhang, Y.: UAV communications for 5G and beyond: recent advances and future trends. IEEE Internet Things **6**(2), 2241–2263 (2018)
2. Popovski, P., Trillingsgaard, K.F., Simeone, O.: 5G wireless network slicing for eMBB, URLLC, and mMTC: a communication-theoretic view. IEEE Access **6**, 55765–55779 (2018)
3. Ning, Z., Dong, P., Wang, X.: Mobile edge computing enabled 5G health monitoring for internet of medical things: a decentralized game theoretic approach. IEEE J. Sel. Area Commun. **39**(2), 463–478 (2021)
4. Xie, R., Lian, X., Jia, Q.: Overview of mobile edge computing offload technology. J. Commun. **39**(11), 138–155 (2018)
5. Cao, S., Lee, V.C.: An accurate and complete performance modeling of the IEEE 802.11 p MAC sublayer for VANET. Comput. Commun. **149**, 107–120 (2020)
6. Ni, S.J., Zhao, J.H.: Key technologies in physical layer of 5G wireless communications network. Telecommun. Sci. **31**(12), 48–53 (2015)
7. Xie, X.Z.: Key requirements and multi-access multiplexing techniques for 5G. CQU Posts Telecommun. **27**(4), 434–440 (2015)
8. Ma, X., Zhao, J., Sun, X., Gong, Y.: Key technologies in collaborative network based on MEC. Telecommun. Sci. **36**(6), 28–37 (2020)
9. Li, N.Z.: Comparison of new multi carrier transmission technologies for 5G. Commun. Technol. **49**(05), 519–523 (2016)
10. Kibria, M.G., Villardi, G.P., Ishizu, K.: Throughput enhancement of multicarrier cognitive M2M networks: universal-filtered OFDM systems. IEEE Internet Things **3**(5), 830–838 (2016)
11. Helwa, S.S., Ibrahim, M., Elramly, S.: Universal filtered multi-carrier performance analysis with multipath fading channels. In: International Conference on Next Generation Mobile Applications, Security and Technologies, Cardiff, pp. 35–40. IEEE Press (2016)
12. Ambatali, C.D.M., Marciano, J.J.S.: Performance evaluation of the UFMC scheme under various transmission impairments. In: 2016 IEEE International Conference on Communication, Surabaya, pp. 24–28. IEEE Press (2016)
13. Wang, X., Wild, T., Schaich, F.: Universal filtered multi-carrier with leakage-based filter optimization. In: European Wireless 2014, European Wireless Conference, Spain, pp. 1–5. VDE Press (2014)
14. Wang, X., Wild, T., Schaich, F.: Filter optimization for carrier-frequency-and timing-offset in universal filtered multi-carrier systems. In: Vehicular Technology Conference, Glasgow, pp. 1–6. IEEE Press (2015)
15. Geng, S., Xiong, X., Cheng, L., et al.: UFMC system performance analysis for discrete narrow-band private networks. In: IEEE 2015 6th International Symposium on Microwave, Antenna, Propagation, and EMC Technologies (MAPE), Shanghai, pp. 303–307. IEEE Press (2015)

16. Yu, X., Gao, Y., Duan, S.: Channel estimation of UFMC system in multipath channel. Telecommun. Sci. **34**(4), 22–30 (2018)
17. Yang, L., He, P., Wang, S.: Carrier frequency synchronization technology in UFMC. Telecommun. Sci. **32**(11), 50–55 (2016)
18. Tang, M.F., Su, B.: Filter optimization of low out-of-subband emission for universal-filtered multicarrier systems. In: IEEE 2016 International Conference on Communications Workshops (ICC), Kuala Lumpur, pp. 468–473. IEEE Press (2016)